

Common Oxygen Binding Site in Hemocyanins from Arthropods and Mollusks. Evidence from Raman Spectroscopy and Normal Coordinate Analysis

Jinshu Ling,^{1a} Lisa P. Nestor,^{1b,c} Roman S. Czernuszewicz,^{1d} Thomas G. Spiro,^{1b} Robert Fraczkiewicz,^{1d} Kamala D. Sharma,^{1a} Thomas M. Loehr,^{1a} and Joann Sanders-Loehr^{*,1a}

Contribution from the Department of Chemistry, Biochemistry, and Molecular Biology, Oregon Graduate Institute of Science and Technology, Portland, Oregon 97291-1000, Department of Chemistry, University of Houston, Houston, Texas 77204, and Department of Chemistry, Princeton University, Princeton, New Jersey 08544

Received April 26, 1994*

Abstract: Resonance Raman (RR) spectra of oxyhemocyanins (oxyHcs) from an arthropod (*Limulus polyphemus*) and two mollusks (*Busycon canaliculatum* and *Octopus dofleini*) exhibit their peroxide-like O–O stretching mode at the unusual low frequency of $\sim 745\text{ cm}^{-1}$. This low energy appears to be indicative of a $\mu\text{-}\eta^2\text{:}\eta^2$ coordination geometry in which a side-on peroxide bridges two Cu(II) ions, as has been observed in the crystal structure of *Limulus* oxyHc (Magnus, K. A.; et al. *Proteins*, in press) and a model compound (Kitajima, N.; et al. *J. Am. Chem. Soc.* **1992**, *114*, 1277–1291). We have now identified a Cu–peroxide stretch, $\nu_{\text{as}}(\text{Cu}_2\text{O}_2)$, at 542 cm^{-1} (519 cm^{-1} in $^{18}\text{O}_2$) and its first overtone, $2\nu_{\text{as}}(\text{Cu}_2\text{O}_2)$, at 1085 cm^{-1} (1039 cm^{-1} in $^{18}\text{O}_2$) in *Octopus* oxyHc. When the protein is oxygenated with $^{16}\text{O}^{18}\text{O}$, only a single $\nu_{\text{as}}(\text{Cu}_2^{16}\text{O}^{18}\text{O})$ mode appears at 529 cm^{-1} . These results provide definitive evidence that the peroxy group is symmetrically bound to the two Cu atoms, as expected for a $\mu\text{-}\eta^2\text{:}\eta^2$ geometry. Similar $\nu_{\text{as}}(\text{Cu}_2\text{O}_2)$ and $2\nu_{\text{as}}(\text{Cu}_2\text{O}_2)$ vibrations are detected in the RR spectra of *Busycon* and *Limulus* Hcs. These findings make it likely that the proteins from both phyla have the same $\mu\text{-}\eta^2\text{:}\eta^2$ copper peroxide structure. In addition, oxyHcs from both phyla have a set of eight distinct vibrational modes between 170 and 370 cm^{-1} . Through the use of normal coordinate analysis, these peaks can be assigned to $\nu_{\text{s}}(\text{Cu}_2\text{O}_2)$ and $\nu_{\text{as}}(\text{Cu}_2\text{O}_2)$ modes coupled with Cu–N(His) stretching vibrations. The extensive coupling with imidazole modes is supported by ^{65}Cu - and D-substitution data for *Busycon* oxyHc. The similarity of the vibrational patterns between the two phyla suggests that molluscan Hcs also have six terminal His ligands at the dinuclear Cu site. The greatest RR intensity is associated with the Cu–N(axial His) stretching mode at $\sim 280\text{ cm}^{-1}$ because the axial His ligands are the most affected by changes in copper oxidation state. This mode may be sensitive to R- and T-state conformations and, thus, serve as an indicator of oxygen affinity.

Introduction

Hemocyanins (Hcs) are copper-containing oxygen-transport proteins found in the hemolymph of mollusks and arthropods, where they occur as multisubunit aggregates.^{2,3} Molluscan Hcs are cylindrical molecules with 10–20 subunits of $\sim 350\,000$ Da. Each subunit, in turn, contains seven or eight covalently linked, $\sim 50\,000$ -Da functional units, each of which contains two copper atoms that can bind one O_2 molecule. Arthropod Hcs are composed of hexamers or oligohexamers built from individual $\sim 75\,000$ -Da subunits in which each subunit also has a dinuclear copper site and binds one oxygen molecule. For the Hcs from both phyla, the deoxygenated form is colorless and in the Cu(I) oxidation state. Reaction with O_2 results in the oxidation of Cu(I) to Cu(II) and the reduction of O_2 to peroxide.⁴ The resulting intensely blue oxyHc exhibits absorption maxima at ~ 345 and $\sim 570\text{ nm}$ that are both assigned as peroxide \rightarrow Cu(II) charge-transfer (CT) transitions.^{4,5}

X-ray crystal structures have been determined for arthropod hemocyanins from the spiny lobster, *Panulirus interruptus*,^{6,7} and the horseshoe crab, *Limulus polyphemus*.⁸ In the deoxy state, each of the Cu(I) atoms is ligated to three histidines with a Cu...Cu separation of 3.5 \AA for *Panulirus* and 4.6 \AA for *Limulus* (see Results and Discussion). Each of the copper atoms has the same ligation pattern with two His residues from an H–X₃–H sequence in one α -helix and the third His from an adjacent α -helix. The pseudo-twofold symmetry within the Cu-binding domain suggests that the protein was formed by duplication and fusion of a gene from an ancestral mononuclear copper site.⁹

For oxyHc from *Limulus*, the crystal structure⁸ shows that the two copper atoms are bridged by a side-on peroxide in a $\mu\text{-}\eta^2\text{:}\eta^2$ geometry with a Cu...Cu separation of 3.6 \AA (Figure 1). Each Cu(II) is square pyramidal. There are four equatorial N(His) in approximately the same plane as the Cu_2O_2 moiety and two axial N(His) ligands at a longer distance, yielding average Cu–N bond lengths of 2.1 and 2.4 \AA , respectively. This type of Cu_2O_2

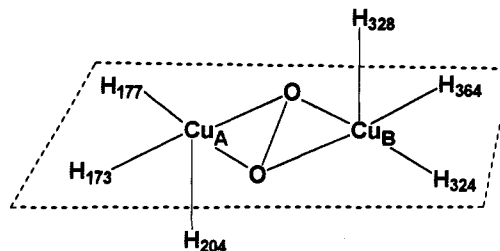


Figure 1. Active site of oxyhemocyanin from *L. polyphemus* subunit II based on the 2.4-\AA resolution crystal structure.⁸

* Abstract published in *Advance ACS Abstracts*, August 1, 1994.

(1) (a) Oregon Graduate Institute of Science and Technology. (b) Princeton University. (c) Present address: Department of Chemistry, College of the Holy Cross, Worcester, MA 01610. (d) University of Houston.

(2) Van Holde, K. E.; Miller, K. I. *Q. Rev. Biophys.* **1982**, *15*, 1–129.

(3) Pr aux, G.; Gielens, C. In *Copper Proteins and Copper Enzymes*; Lontie, R., Ed., CRC Press: Boca Raton, FL, 1984; Vol. II, pp 160–198.

(4) Freedman, T. B.; Loehr, J. S.; Loehr, T. M. *J. Am. Chem. Soc.* **1976**, *98*, 2809–2815.

(5) (a) Eickman, N. C.; Himmelwright, R. S.; Solomon, E. I. *Proc. Natl. Acad. Sci. U.S.A.* **1979**, *76*, 2094–2098. (b) Ross, P. K.; Solomon, E. I. *J. Am. Chem. Soc.* **1991**, *113*, 3246–3259. (c) Solomon, E. I.; Tuzcek, F.; Root, D. E.; Brown, C. A. *Chem. Rev.* **1994**, *94*, 827–856.

(6) Volbeda, A.; Hol, W. G. J. *J. Mol. Biol.* **1989**, *209*, 249–279.

coordination was first observed in the model compound $[\text{Cu-HB}(3,5\text{-}i\text{-Pr}_2\text{pz})_3]_2(\text{O}_2)$, which also binds O_2 reversibly and has spectral characteristics similar to those of oxyHc.^{10,11} The $\mu\text{-}\eta^2/\eta^2$ -peroxide geometry had also been proposed for a series of $[\text{Cu}_2(\text{NPY}_2)_2(\text{O}_2)]^{2+}$ complexes on the basis of EXAFS measurements and the appearance of the expected absorption bands.¹² These two sets of cupric peroxide model compounds have Cu...Cu separations of 3.6 and 3.2–3.4 Å, respectively.

There is, as yet, no crystal structure available for any molluscan hemocyanin. The similarity of the spectroscopic and magnetic properties of arthropod and molluscan Hcs indicates that they have similar dinuclear copper sites.¹³ EXAFS measurements of deoxyHcs reveal that each copper is complexed by two or three His residues and that the Cu...Cu distance is 3.43–3.48 Å in the proteins from both phyla.¹⁴ Molluscan Hcs¹⁵ exhibit sequence identity to arthropod Hcs and tyrosinases^{16a} in a region corresponding to the Cu B site (Figure 1). For example, in *Octopus dofleini* Hc (functional unit g), His 174, 178, and 205 are suggested to be ligands to Cu B, and they could well arise from an H-X₃-H sequence on one helix and a third His on an adjacent helix.¹⁵ In contrast, the Cu A' site of molluscan Hcs is related to the Cu A' site of tyrosinases but bears no sequence similarity to the Cu A site of arthropod Hcs. Two His residues (46 and 74 of *Octopus* Hc) are conserved in all molluscan Hcs and tyrosinases and, thus, are likely to be ligands to Cu A'.¹⁶ A third His (residue 65 in *Octopus* Hc) is conserved in the cDNA sequences of all molluscan Hcs and tyrosinases but has been shown to be modified by a thioether bond between the n-2 Cys (63 in *Octopus* Hc) and the C2 of the imidazole ring in *Helix pomatia* (mollusk) Hc and *Neurospora crassa* tyrosinase.¹⁷ Each of these three His residues in the CuA' domain has been implicated as a Cu ligand in *Streptomyces glaucescens* tyrosinase by site-directed mutagenesis.^{16b,c} Thus, these three His residues are likely to be CuA' ligands in other tyrosinases as well as in molluscan Hcs. Further evidence in support of this hypothesis is given below.

Resonance Raman (RR) spectroscopy is a useful technique for providing more definitive information about the structure of Cu_2O_2 sites.¹⁸ Previous RR studies detected an O–O stretching vibration, $\nu(\text{O}-\text{O})$, at $\sim 750\text{ cm}^{-1}$ in oxyHcs from both mollusks and arthropods.^{4,19} This vibrational frequency is indicative of a

peroxide, and the assignment is supported by the $\sim 40\text{-cm}^{-1}$ shift to lower energy for protein prepared in $^{18}\text{O}_2$. The observation of only a single $\nu(\text{O}-\text{O})$ peak for the $^{16}\text{O}^{18}\text{O}$ complex of molluscan Hc from *Busycon canaliculatum*²⁰ suggests that the two oxygen atoms are equivalent and bound in a symmetric manner, as expected for a $\mu\text{-}\eta^2:\eta^2$ peroxide.

We have now, for the first time, identified a $\nu_{\text{as}}(\text{Cu}_2\text{O}_2)$ mode at $\sim 545\text{ cm}^{-1}$ and its first overtone $2\nu_{\text{as}}(\text{Cu}_2\text{O}_2)$ at $\sim 1090\text{ cm}^{-1}$ in oxyHc from the arthropod *Limulus* as well as from the mollusks *Octopus* and *Busycon*. These results provide strong evidence that oxyHcs from both phyla have the same $\mu\text{-}\eta^2:\eta^2$ peroxide structure. The RR spectrum of *Octopus* Hc prepared from $^{16}\text{O}^{18}\text{O}$ reveals only a single $\nu_{\text{as}}(\text{Cu}_2^{16}\text{O}^{18}\text{O})$ vibration, thereby proving unequivocally that the peroxide is bound to the copper ions in a symmetric fashion. The Cu–N(His) vibrations in the 170–370- cm^{-1} region of the RR spectrum of *Busycon* oxyHc¹⁹ have now been rigorously assigned using $^{63/65}\text{Cu}$ and deuterium isotope shifts and normal coordinate analysis. The molluscan and arthropod Hcs show a similar pattern of Cu–N(His) vibrations, making it likely that the Hcs from the two phyla have the same set of terminal copper ligands.

Experimental and Computational Procedures

Protein Samples. *O. dofleini* hemolymph was generously provided by Dr. Karen Miller (Oregon State University).²¹ The hemocyanin was purified by ultracentrifugation for 2 h at 55 000 rpm (Ti 65 rotor, Beckman). The pellet was dissolved in 0.1 M Tris-HCl, 50 mM MgCl_2 , 10 mM CaCl_2 (pH 7.8) by incubating overnight at 5 °C. The concentration of oxyHc was determined by $\epsilon_{345} = 10\,000\text{ M}^{-1}\text{ cm}^{-1}$ per Cu.²¹ This protein could be stored for several months at $-80\text{ }^\circ\text{C}$ without affecting the quality of either the electronic or the Raman spectrum.

B. canaliculatum hemocyanin was prepared from the hemolymph of the mollusk designated as *Busycotypus* (Marine Biological Laboratory, Woods Hole, MA), as described previously.^{4,19} After a brief centrifugation at 12 000g, the protein was dialyzed versus 0.05 M sodium carbonate (pH 9.8) to cause dissociation into subunits. This lowered the turbidity and allowed the protein to be concentrated to $\sim 5\text{ mM}$ in Cu by ultrafiltration in a Centricon 30 (Amicon) device. The oxyHc concentration was determined from $\epsilon_{347} = 10\,000\text{ M}^{-1}\text{ cm}^{-1}$ per Cu.¹³

L. polyphemus hemocyanin was generously provided by Dr. Celia Bonaventura (Duke University Marine Laboratory, Beaufort, NC) and further purified as published.²² The Hc was first dissociated into subunits by dialysis versus 0.05 M Tris-HCl, 0.05 M glycine, 0.01 M EDTA, and 0.1 M NaCl (pH 8.9), then applied to a DEAE Sepharose CL-6B column (Pharmacia, 1.5 × 25 cm) in the same buffer, and eluted with a 500-mL linear gradient of 0.2–0.5 M NaCl. Subunit II, which eluted at 0.23 M NaCl, was concentrated using Centriprep and Centricon (Amicon) ultrafiltration devices. The oxyHc concentration was determined from $\epsilon_{340} = 12\,000\text{ M}^{-1}\text{ cm}^{-1}$ per Cu.²²

O_2 Isotope Exchange. *Octopus* oxyHc (4 mM in Cu) was flushed with carbon monoxide in a gas-delivery apparatus²³ until the blue color of the oxygenated protein disappeared. Excess CO was removed by evacuating the system. The protein was then reoxygenated by exposure to $^{18}\text{O}_2$ (99 atom %, ICON) or $^{16}\text{O}^{18}\text{O}$ (50% ^{18}O , Cambridge Isotope Laboratory) for 5 min, with reappearance of the characteristic blue color.

Deuterium Exchange. *Busycon* oxyHc (5 mL) was centrifuged as described above for *Octopus* Hc, and the $\sim 0.1\text{-mL}$ pellet was dissolved in 5 mL of 0.05 M carbonate buffer in D_2O (99.8 atom %, Aldrich) at a pH reading of 9.8. The protein was cycled through the deoxy state by flushing with buffer-equilibrated argon for 6 h. The sample was reconcentrated by centrifugation and the $\sim 0.1\text{-mL}$ pellet dissolved in 0.1 mL of D_2O buffer. A control sample was prepared in parallel in H_2O .

(7) Volbeda, A.; Feiters, M. C.; Vincent, M. G.; Bouwman, E.; Dobson, B.; Kalk, K. H.; Reedijk, J.; Hol, W. G. *J. Eur. J. Biochem.* **1989**, *181*, 669–673.

(8) (a) Magnus, K. A.; Ton-That, H.; Carpenter, J. E. In *Bioinorganic Chemistry of Copper*; Karlin, K. D., Tyeklar, Z., Eds.; Chapman and Hall: New York, 1993; pp 143–150. (b) Magnus, K. A.; Hazes, B.; Ton-That, H.; Bonaventura, C.; Bonaventura, J.; Hol, W. G. *J. Proteins* **1994**, *19*, 302–309. (c) Hazes, B.; Magnus, K. A.; Bonaventura, C.; Bonaventura, J.; Dauter, Z.; Kalk, K. H.; Hol, W. G. *Protein Sci.* **1993**, *2*, 597–619.

(9) Volbeda, A.; Hol, W. G. *J. Mol. Biol.* **1989**, *206*, 531–546.

(10) (a) Kitajima, N.; Fujisawa, K.; Fujimoto, C.; Moro-oka, Y.; Hashimoto, S.; Kitagawa, T.; Toriumi, K.; Tatsumi, K.; Nakamura, A. *J. Am. Chem. Soc.* **1992**, *114*, 1277–1291. (b) Kitajima, N.; Moro-oka, Y. *Chem. Rev.* **1994**, *94*, 737–757.

(11) Baldwin, M. J.; Root, D. E.; Pate, J. E.; Fujisawa, K.; Kitajima, N.; Solomon, E. I. *J. Am. Chem. Soc.* **1992**, *114*, 10421–10431.

(12) (a) Karlin, K. D.; Haka, M. S.; Cruse, R. W.; Meyer, G. J.; Farooq, A.; Gultneh, Y.; Hayes, J. C.; Zubieta, J. *J. Am. Chem. Soc.* **1988**, *110*, 1196–1207. (b) Blackburn, N. J.; Strange, R. W.; Farooq, A.; Haka, M. S.; Karlin, K. D. *J. Am. Chem. Soc.* **1988**, *110*, 4263–4272.

(13) Himmelwright, R. S.; Eickman, N. C.; LuBien, C. D.; Solomon, E. I. *J. Am. Chem. Soc.* **1980**, *102*, 5378–5388.

(14) (a) Brown, J. M.; Powers, L.; Kincaid, B.; Larrabee, J. A.; Spiro, T. G. *J. Am. Chem. Soc.* **1980**, *102*, 4210–4216. (b) Woolery, G. L.; Powers, L.; Winkler, M.; Solomon, E. I.; Spiro, T. G. *J. Am. Chem. Soc.* **1984**, *106*, 86–92.

(15) (a) Lang, W. H.; van Holde, K. E. *Proc. Natl. Acad. Sci. U.S.A.* **1991**, *88*, 244–248. (b) Lang, W. H. *Biochemistry* **1988**, *27*, 7276–7282.

(16) (a) Lerch, K.; Huber, M.; Schneider, H.-J.; Drexel, R.; Linzen, B. *Inorg. Biochem.* **1986**, *26*, 213–217. (b) Huber, M.; Lerch, K. *Biochemistry* **1988**, *27*, 5610–5615. (c) Jackman, M.; Hajnal, A.; Lerch, K. *Biochem. J.* **1991**, *274*, 707–713.

(17) (a) Gielens, C.; De Geest, N.; Xin, X.-Q.; Pr aux, G. *Arch. Int. Physiol. Biochem. Biophys.* **1994**, *102*, B11. (b) Lerch, K. *J. Biol. Chem.* **1982**, *257*, 6414–6419.

(18) Loehr, T. M.; Shlemke, A. K. In *Biological Applications of Raman Spectroscopy*; Spiro, T. G., Ed.; Wiley: New York, 1988; Vol. 3, pp 439–490.

(19) (a) Larrabee, J. A.; Spiro, T. G. *J. Am. Chem. Soc.* **1980**, *102*, 4217–4223. (b) Larrabee, J. A.; Spiro, T. G.; Ferris, N. S.; Woodruff, W. H.; Maltese, W. A.; Kerr, M. S. *J. Am. Chem. Soc.* **1977**, *99*, 1979–1980.

(20) Thammann, T. J.; Loehr, J. S.; Loehr, T. M. *J. Am. Chem. Soc.* **1977**, *99*, 4187–4189.

(21) (a) Miller, K. I.; van Holde, K. E. *Comp. Biochem. Physiol.* **1982**, *73B*, 1013–1018. (b) Miller, K. I.; van Holde, K. E.; Tourmadje, A.; Johnson, W. C., Jr.; Larry, J. *Biochemistry* **1988**, *27*, 7282–7288.

(22) Brenowitz, M.; Bonaventura, C.; Gianazza, E. *Arch. Biochem. Biophys.* **1981**, *210*, 748–761.

(23) Loehr, T. M.; Sanders-Loehr, J. *Methods Enzymol.* **1993**, *226*, 431–470.

Table 1. Resonance Raman Spectra of Oxyhemocyanins and a Model Compound^a

<i>Octopus</i> Hc ^b			<i>Busycon</i> Hc ^c				<i>Limulus</i> Hc ^d		μ - η^2 - η^2 model ^e		assignment ^f		
ν	$\Delta^{18}\text{O}_2$	$\Delta^{16}\text{O}^{18}\text{O}$	ν	$\Delta^{18}\text{O}_2$	$\Delta^{65}\text{Cu}$	$\Delta\text{D}_2\text{O}$	$\Delta\text{H}_2^{18}\text{O}$	ν	$\Delta^{18}\text{O}_2$	ν	$\Delta^{18}\text{O}_2$	PED	sym
1085	-46		1093					1087		1144	-42	$2\nu_{\text{as}}(\text{Cu}_2\text{O}_2)$	
749	-40	-19	749	41		0	0	744	-39 ^g	763	-40	$\nu(\text{O}-\text{O})$	A _g
								570				$\nu_{\text{as}}(\text{Cu}_2\text{O}_2)$	B _u
542	-23	-13	547			0	0	543		572 ^h	-21 ^h	$\nu_{\text{as}}(\text{Cu}_2\text{O}_2)$	B _g
342	0		345		-1	-1	0	363				$\nu_{\text{s}}(\text{Cu}-\text{N}_{\text{eq}})$	A _g
314	0		314		-2	-2	0	336				$\nu_{\text{as}}(\text{Cu}-\text{N}_{\text{eq}})$	A _u
294	0		293		-2	0	0	303				$\nu_{\text{as}}(\text{Cu}-\text{N}_{\text{eq}})$	B _u
285			289		-2			313				$\nu_{\text{as}}(\text{Cu}-\text{N}_{\text{eq}})$	B _g
270	0		270		-2	-1	0	286		284	0	$\nu_{\text{s}}(\text{Cu}-\text{N}_{\text{ax}})$	A _g
237			240					224				$\nu_{\text{as}}(\text{Cu}_2\text{O}_2)$	A _u
228	0		229		-2	-1	0	265				$\nu_{\text{as}}(\text{Cu}-\text{N}_{\text{ax}})$	B _u
174	0		174		0	0	0	190				$\nu_{\text{s}}(\text{Cu}_2\text{O}_2)$	A _g

^a Frequency in cm^{-1} . Isotope shift (Δ) in presence of heavier isotope. ^b *O. dofleini* Hc data were obtained at 15 K, except for the 750- cm^{-1} peak at 278 K (Jarrell-Ash). Isotope shifts relative to $^{16}\text{O}_2$ preparation. ^c *B. canaliculatum* Hc. Data for $^{16}\text{O}_2/^{18}\text{O}_2$ at 298 K from ref 4. Data for $^{63}\text{Cu}/^{65}\text{Cu}$ obtained at 77 K (Spex). Data for $\text{H}_2\text{O}/\text{D}_2\text{O}$ and $\text{H}_2\text{O}/\text{H}_2^{18}\text{O}$ obtained at 15 K (Jarrell-Ash) on samples cycled through the deoxy state. ^d *L. polyphemus* Hc subunit II data at 15 K, except for the 744- cm^{-1} peak at 278 K (Jarrell-Ash). ^e Data for $[\text{CuHB}(3,5\text{-Ph}_2\text{pz})_3]_2(\text{O}_2)$ from ref 11. ^f Major PED contributor to each mode and symmetry based on NCA for *Busycon* oxyHc (Table 3, below). N_{ax} = axial His; N_{eq} = equatorial His. ^g Reference 30. ^h Not observed. Frequencies calculated from $2\nu_{\text{as}}(\text{Cu}_2\text{O}_2)$.

Alternatively, the exchange was performed using three or four rounds of 10-fold dilution in D_2O buffer and concentration by ultrafiltration. These two methods gave similar RR results.

H_2^{18}O Exchange. *Busycon* oxyHc in 0.05 mM carbonate (pH 9.8) was concentrated in a Centricon 30 to 8 mM in Cu and then diluted fivefold with pH 9.8 buffer prepared in H_2^{16}O or H_2^{18}O (97 atom % ^{18}O , YEDA, Israel). This procedure was repeated for a second time. The oxyHc was then converted to deoxyHc by flushing for 30 min with CO gas and incubated for 12 h. Samples were then bubbled with O_2 gas for 10 min to allow reoxygenation and were reconcentrated by ultrafiltration. The filtrate of the H_2^{18}O sample contained 80% ^{18}O according to a mass spectral analysis.

^{65}Cu Exchange. *Busycon* apoHc was prepared by dialysis against KCN and reconstituted with ^{63}Cu (99.89%) or ^{65}Cu (99.7%, Oak Ridge National Laboratories) as described previously.¹⁹

Raman Spectroscopy. Some of the Raman spectra were recorded on a Jarrell-Ash spectrometer at the Oregon Graduate Institute using an RCA C31034 photomultiplier and an ORTEC model 9302 amplifier-discriminator and interfaced with an Intel 310 computer. Excitation sources were Spectra-Physics 164-05 (Ar^+) and 2025-11 (Kr^+) lasers. Spectra were obtained on samples in capillaries in a Dewar maintained at either 278 or 90 K or on samples frozen onto the cold head of a Displex (Air Products) at 15 K, all in a 150° backscattering geometry.²³ Other Raman spectra were recorded on a Spex 1401 spectrometer at Princeton University using an RCA C31034A photomultiplier and photon-counting electronics and interfaced to a DEC MINC computer. The excitation source was a Kr^+ laser (356.4 nm), and the spectra were obtained at 77 K as described previously.²⁴

Normal Coordinate Analysis. Normal mode calculations were performed with the GF matrix method²⁵ and a general valence force field which included bond stretching, angle bending, and torsional force constants. Also included were valence interaction force constants for all coordinates sharing at least one atom. Molecular parameters for the $\text{Cu}_2\text{O}_2(\text{Im})_6$ units of *Busycon* and *Limulus* Hcs were based on the crystal structure data for *Limulus* oxyHc,^{8b} from which Cartesian coordinates were determined by simple trigonometric relationships, holding the Cu_2O_2 rhombus planar and all bond lengths constant to maintain C_{2h} symmetry (with the C_2 axis along the O-O bond). Only atoms in the first coordination sphere were included in the calculations, and the histidine nitrogens were treated as point masses of 67 amu, the full mass of the imidazole ring. A redesigned NCA program package based on Schachtschneider's algorithms²⁶ and a newly developed procedure²⁷ for refinement of the harmonic vibrational force fields, was used to construct the G matrices, to solve the secular equations $|\text{GF} - E\lambda| = 0$ for each symmetry species, and to determine the force constants. This new algorithm effectively minimizes regularization error during a least-squares iterative

refinement and is immune to convergence problems.³³ All normal mode computations were carried out on a Jetson VAX-X cluster computer at the University of Houston. Normal eigenvectors were generated by transferring the Cartesian atomic displacements from the NCA calculations into molecular graphics software, X-mole,²⁸ on an INDY (Silicon Graphics) workstation.

Results and Discussion

$\nu(\text{O}-\text{O})$ Vibration. Previous studies of oxyHc from the mollusk *Busycon* have shown that excitation within either the 570- or 345-nm absorption band leads to enhancement of the peroxide O-O stretch at 749 cm^{-1} .^{4,18,19} This vibrational mode shifts to 728 cm^{-1} when the sample is prepared with $^{16}\text{O}^{18}\text{O}$ and to 708 cm^{-1} with $^{18}\text{O}_2$.^{4,20} The appearance of only a single $\nu(\text{O}-\text{O})$ mode for the mixed isotope $^{16}\text{O}^{18}\text{O}$ suggests that the two oxygen atoms of the bound peroxide are equivalent.²⁰ The failure to observe any shift in $\nu(\text{O}-\text{O})$ after incubation of *Busycon* Hc in D_2O (Table 1) indicates that the bound peroxide is neither protonated nor H-bonded to solvent or to any other proton donor.

Similar results have now been obtained for oxyHc from the mollusk *Octopus*. Excitation within the 570-nm absorption band yields an intense peak at 749 cm^{-1} (Figure 2A) that shifts to 709 cm^{-1} in $^{18}\text{O}_2$ (Figure 2C). This 40- cm^{-1} isotopic shift in $^{18}\text{O}_2$ is similar to those previously reported for *Busycon* (mollusk) and *Cancer magister* (arthropod) Hcs¹⁸ and definitively identifies the 749- cm^{-1} feature of *Octopus* Hc as the O-O stretch of peroxide. The broad feature centered at ~ 755 cm^{-1} in Figure 2C consists of two bands, one due to residual $^{16}\text{O}_2$ at 749 cm^{-1} and the other due to a protein band (most likely tryptophan²⁹) at ~ 760 cm^{-1} . A more prominent protein peak at 760 cm^{-1} is observed for *Octopus* Hc reacted with an isotopic mixture containing $\sim 50\%$ $^{16}\text{O}^{18}\text{O}$ (Figure 2B) due to the incomplete reoxygenation of the sample. Nevertheless, the RR spectrum exhibits distinct new features at 709 and 730 cm^{-1} attributable to $\nu(^{18}\text{O}-^{18}\text{O})$ and $\nu(^{16}\text{O}-^{18}\text{O})$, respectively. The $\nu(^{16}\text{O}-^{18}\text{O})$ frequency is close to the values of 728- and 725- cm^{-1} observed previously for *Busycon* and *Limulus* oxyHcs.^{20,30}

There appears to be only a single $\nu(^{16}\text{O}-^{18}\text{O})$ species responsible for the 730- cm^{-1} peak of *Octopus* Hc (Figure 2B). It has a similar width to the $\nu(^{18}\text{O}-^{18}\text{O})$ mode at 709 cm^{-1} and twice the intensity, as expected from the isotope composition of the sample. The observation of a single $\nu(^{16}\text{O}-^{18}\text{O})$ vibrational mode, as is also the case for *Busycon* and *Limulus* Hcs,^{20,30} suggests that the two peroxide oxygen atoms are equivalent. However, the O-O stretch

(24) Czernuszewicz, R. S.; Johnson, M. K. *Appl. Spectrosc.* **1983**, *37*, 297-298.

(25) Wilson, E. B.; Decius, J. C.; Cross, P. C. *Molecular Vibrations*; McGraw-Hill: New York, 1955.

(26) Schachtschneider, J. H. Technical Report Nos. 51-56 and 231-264; Shell Development Company: Emeryville, CA, 1962.

(27) Fraczkiewicz, R.; Czernuszewicz, R. S. To be submitted.

(28) X-mole, version 1.3.1; Minnesota Supercomputer Center, Inc.: Minneapolis, MN, 1993.

(29) Lord, R. C.; Yu, N.-T. *J. Mol. Biol.* **1970**, *50*, 509-524.

(30) Kurtz, D. M., Jr. Ph.D. Dissertation, Northwestern University, 1977.

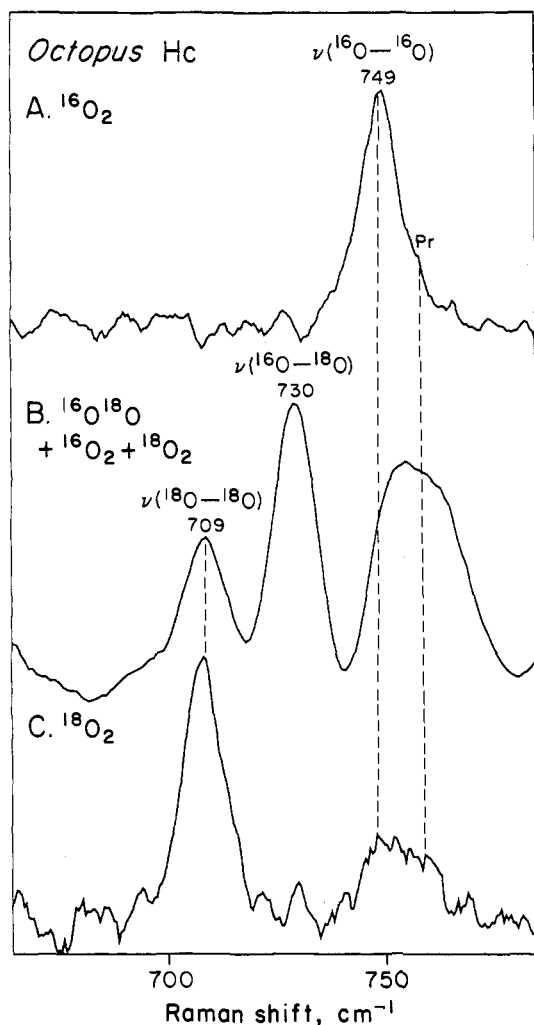


Figure 2. RR spectra of Hc from *O. dofleini* oxygenated with (A) $^{16}\text{O}_2$, (B) mixed-isotope O_2 , and (C) $^{18}\text{O}_2$. The mixed-isotope O_2 contained 0.4 $^{18}\text{O}_2$ /1.0 $^{16}\text{O}^{18}\text{O}$ /0.6 $^{16}\text{O}_2$ according to the Raman spectrum of the gas. Spectra were obtained on a Jarrell-Ash instrument, with samples (4 mM in Cu) in sealed capillaries at 278 K, using the following conditions for excitation, spectral resolution, scan rate, and repetitive scanning: (A) 530.9 nm (25 mW), 8 cm^{-1} , $1\text{ cm}^{-1}\text{ s}^{-1}$, 7 scans; (B) 514.5 nm (40 mW), 8 cm^{-1} , $0.5\text{ cm}^{-1}\text{ s}^{-1}$, 50 scans; (C) 514.5 nm (30 mW), 8 cm^{-1} , $1\text{ cm}^{-1}\text{ s}^{-1}$, 4 scans. Pr = protein mode.

is a relatively pure mode showing little dependence on peroxide coordination geometry. Normal coordinate analysis for an end-on-bound peroxide with clearly inequivalent oxygens leads to a predicted splitting of only 5 cm^{-1} for the two $\nu(^{16}\text{O}-^{18}\text{O})$ modes.³¹ A mixed-isotope splitting of 5 cm^{-1} has been detected for the end-on peroxide at the dinuclear iron center of oxyhemerythrin³² but not for the end-on peroxide in the $[\text{Cu}_2(\text{XYL}-\text{O}-)(\text{O}_2)]^{2+}$ model complex due to poorer spectral resolution.³¹ For this reason, mixed-isotope results based on the O-O stretch may not be definitive. The Cu-O stretch (*vide infra*) provides much stronger evidence with regard to oxygen atom equivalence in coordinated peroxides.

$\nu(\text{Cu}_2\text{O}_2)$ Vibrations. Excitation of molluskan (*Octopus*, *Busycon*) and arthropod (*Limulus*) Hcs within the 345-nm absorption band yields a broad and intense feature at $\sim 1090\text{ cm}^{-1}$ and a weaker band at $\sim 545\text{ cm}^{-1}$ (Figure 3). The band at $\sim 1090\text{ cm}^{-1}$ was originally suggested to be due to an electronic singlet \rightarrow triplet transition associated with the antiferromagnetically coupled Cu^{2+} centers.¹⁹ However, the newly detected

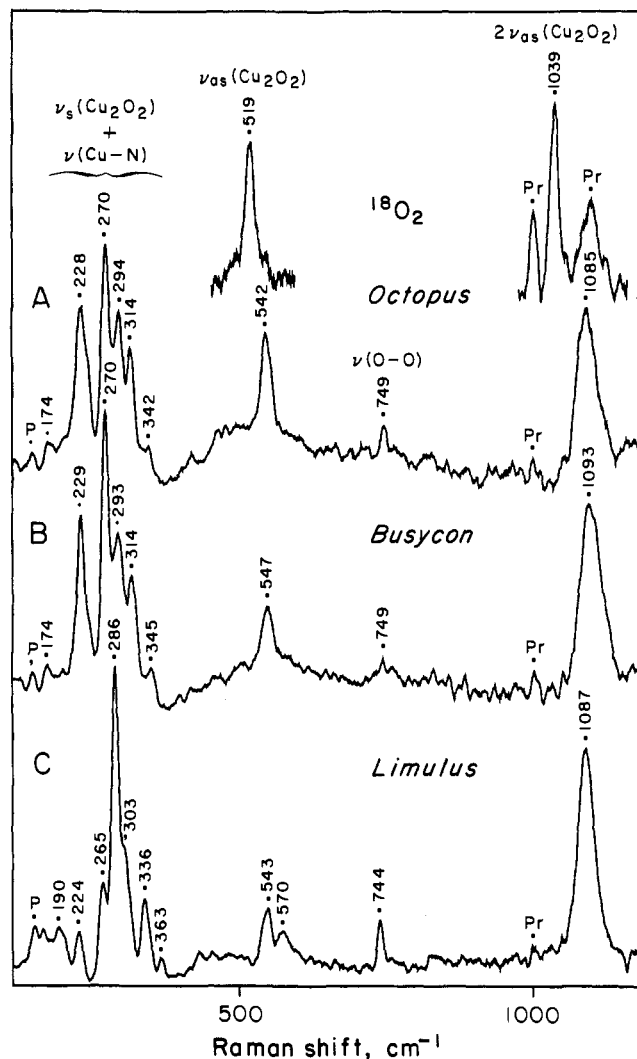


Figure 3. RR spectra of oxyHc from (A) *O. dofleini*, (B) *B. canaliculatum*, and (C) *L. polyphemus* subunit II. Spectra were obtained on a Jarrell-Ash instrument with samples at 15 K using 350.7-nm excitation (30 mW) and the following conditions for [Cu], spectral resolution, scan rate, and repetitive scanning: (A) 2.7 mM, 8 cm^{-1} , $0.5\text{ cm}^{-1}\text{ s}^{-1}$, 6 scans; (B) 5.3 mM, 8 cm^{-1} , $0.5\text{ cm}^{-1}\text{ s}^{-1}$, 8 scans; (C) 2 mM, 8 cm^{-1} , $0.5\text{ cm}^{-1}\text{ s}^{-1}$, 5 scans. The upper traces in A are for Hc oxygenated with $^{18}\text{O}_2$. P = plasma line, Pr = protein Phe ring mode at 1004 cm^{-1} and C-N bend at 1109 cm^{-1} .²⁵

RR mode at $\sim 545\text{ cm}^{-1}$ is at exactly half the frequency of the $\sim 1090\text{-cm}^{-1}$ mode. Moreover, when *Octopus* Hc is oxygenated with $^{18}\text{O}_2$, the peaks at 542 and 1085 cm^{-1} shift by -23 and -46 cm^{-1} , respectively, maintaining their 1:2 frequency relationship (Figure 3A). These two peaks are therefore assigned to a copper-peroxide stretching vibration $\nu(\text{Cu}_2\text{O}_2)$ and its first overtone $2\nu(\text{Cu}_2\text{O}_2)$. The fact that the overtone is considerably more intense than the fundamental suggests that the fundamental is an asymmetric mode and, thus, weakly enhanced. The overtone is, of course, totally symmetry allowed.³³ The observation of resonance-enhanced $\nu_{\text{as}}(\text{Cu}_2\text{O}_2)$ vibrations with UV excitation provides strong supporting evidence for the assignment of the 345-nm absorption band to peroxide \rightarrow Cu(II) CT.⁵

Significantly, the same $\nu_{\text{as}}(\text{Cu}_2\text{O}_2)$ and $2\nu_{\text{as}}(\text{Cu}_2\text{O}_2)$ modes are present in molluskan *Busycon* Hc (Figure 3B) and in arthropod *Limulus* Hc (Figure 3C). The latter spectrum was obtained on subunit II of *Limulus* Hc, whose X-ray crystal structure⁸ has revealed a $\mu\text{-}\eta^2\text{-}\eta^2$ side-on peroxide (Figure 1). The observation of a similar set of Cu-peroxide vibrational modes in the two molluskan Hcs makes it highly likely that they also bind peroxide

(31) Pate, J. E.; Cruse, R. W.; Karlin, K. D.; Solomon, E. I. *J. Am. Chem. Soc.* **1987**, *109*, 2624-2630.

(32) Kurtz, D. M., Jr.; Shriver, D. F.; Klotz, I. M. *J. Am. Chem. Soc.* **1976**, *98*, 5033-5035.

(33) Clark, R. J. H.; Stewart, B. *Struct. Bonding (Berlin)* **1979**, *36*, 1-80.

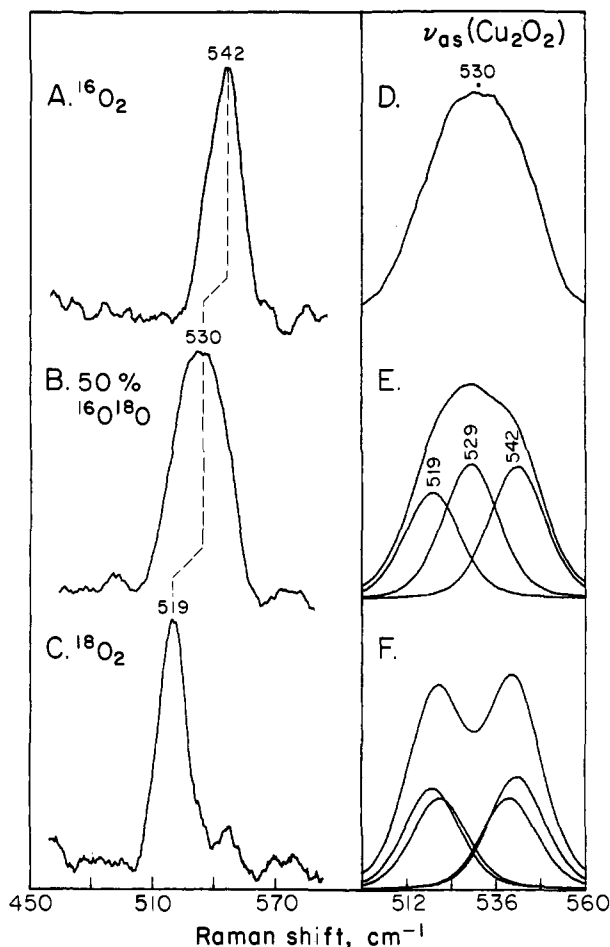


Figure 4. RR spectra of *Octopus* Hc oxygenated with (A) $^{16}\text{O}_2$, (B) mixed-isotope O_2 , and (C) $^{18}\text{O}_2$ with samples as in Figure 2. Spectra were obtained on a Jarrell-Ash instrument with samples at 90 K using 350.7-nm excitation (18 mW) with a spectral resolution of 12 cm^{-1} and scan rate of $0.5\text{ cm}^{-1}\text{ s}^{-1}$. Spectra A, B, and C are averages of 8, 25, and 8 scans, respectively. (D) Expanded plot of B. (E) Simulated spectral envelope for a symmetric peroxide with three components at 519, 529, and 542 cm^{-1} using a full width at half-height (fwhh) of 17.5 cm^{-1} and an intensity ratio of 0.6:1.0:0.8. (F) Simulated spectral envelope for an asymmetric peroxide with four components at 520, 522, 540, and 542 cm^{-1} using a fwhh of 17.5 cm^{-1} and an intensity ratio of 0.6:0.5:0.5:0.7.

in a $\mu\text{-}\eta^2\text{:}\eta^2$ fashion. This conclusion is supported by the finding that the $[\text{CuHB}(3,5\text{-Ph}_2\text{pz})_3]_2(\text{O}_2)$ model compound¹¹ with its $\mu\text{-}\eta^2\text{:}\eta^2$ peroxide exhibits a broad and intense $2\nu_{\text{as}}(\text{Cu}_2\text{O}_2)$ mode at 1144 cm^{-1} that shifts by -46 cm^{-1} with $^{18}\text{O}_2$ (Table 1). This intense overtone has not been detected in the RR spectra of dimeric Cu(II) complexes with η^1 end-on peroxides.^{31,34}

Further evidence in support of $\mu\text{-}\eta^2\text{:}\eta^2$ peroxide coordination in molluscan Hc comes from the use of a mixed isotope of O_2 containing $\sim 50\%$ $^{16}\text{O}^{18}\text{O}$ as in Figure 2B. Using UV excitation, the RR spectrum of *Octopus* hemocyanin in the $\nu_{\text{as}}(\text{Cu}_2\text{O}_2)$ region shows a feature at 530 cm^{-1} (Figure 4B, expanded in 4D) which is considerably broader than that in either of the pure isotopes (Figures 4A and C). The mixed-isotope spectrum (Figure 4D) can be simulated (Figure 4E) with three peaks at 519, 529, and 542 cm^{-1} with relative ratios similar to the initial O_2 gas composition. These peaks are assigned as $\nu_{\text{as}}(\text{Cu}_2^{18}\text{O}_2)$, $\nu_{\text{as}}(\text{Cu}_2^{16}\text{O}^{18}\text{O})$, and $\nu_{\text{as}}(\text{Cu}_2^{16}\text{O}_2)$, respectively, of a symmetrically bound peroxide. If only one end of the peroxide were coordinated to Cu, as in an η^1 end-on configuration, then the two different Cu–O stretching modes ($\text{Cu}\text{-}^{18}\text{O}^{16}\text{O}$ and $\text{Cu}\text{-}^{16}\text{O}^{18}\text{O}$) would have given rise to a spectrum as simulated in Figure 4F. This type of

spectrum has been observed for the end-on peroxides in the $[\text{Cu}_2\text{-}(\text{XYL-O-})(\text{O}_2)]^{2+}$ complex³¹ and in oxyhemerythrin,³² where the $\nu(\text{M}\text{-}^{18}\text{O}^{16}\text{O})$ and $\nu(\text{M}\text{-}^{16}\text{O}^{18}\text{O})$ modes are split by 18 and 16 cm^{-1} , respectively. The absence of such a splitting for $\nu_{\text{as}}(\text{Cu}_2\text{O}_2)$ in *Octopus* Hc is conclusive proof of equivalent oxygen atoms.

Although the $2\nu_{\text{as}}(\text{Cu}_2\text{O}_2)$ mode is observed in both proteins and models containing a $\mu\text{-}\eta^2\text{:}\eta^2$ peroxide, the RR spectrum of $[\text{CuHB}(3,5\text{-Ph}_2\text{pz})_3]_2(\text{O}_2)$ lacks the $\nu_{\text{as}}(\text{Cu}_2\text{O}_2)$ fundamental. The observation of this asymmetric mode in the protein RR spectra indicates that the Cu_2O_2 structure is less symmetric in oxyHc than in the $\mu\text{-}\eta^2\text{:}\eta^2$ model compound. Such a lowering of symmetry in proteins compared to models is a common feature of metalloprotein active sites. Since the arthropod and molluscan Hcs (particularly *Limulus* and *Busycon*) have similar intensities for ν_{as} relative to $2\nu_{\text{as}}$ (Figure 3), molluscan Hc is likely to have the same Cu_2O_2 geometry including a similar symmetry lowering relative to the model compound.

$\nu(\text{Cu}\text{-L})$ Vibrations. Excitation of oxyHc within the 345-nm absorption band also produces a set of eight vibrational features between 170 and 370 cm^{-1} (Figure 3, Table 1). These modes are distinguished from the higher energy modes between 540 and 1100 cm^{-1} by their lack of sensitivity to isotopes of O_2 (Table 1). Earlier RR studies of *Busycon* Hc revealed that the bands at 227, 267, and 287 cm^{-1} were affected by Cu isotope substitution whereas the bands at 227 and 267 cm^{-1} were affected by exchange with D_2O .¹⁹ The latter two bands were assigned to Cu–N(His) stretching, since the NH proton of imidazole is capable of solvent exchange. The low energy of the Cu–N(His) stretch is due to the entire imidazole ring behaving as an oscillator with a point mass of 67. Whether other less intense peaks are also sensitive to isotope exchange was unclear due to the low resolution of spectra obtained at 298 K.

We have been able to obtain higher quality spectra by freezing samples at 77 or 15 K. The spectral improvement is due in part to peak sharpening at low temperature and in part to decreased sample deterioration during UV irradiation. Expanded and higher-resolution spectra of the low-frequency region are shown in Figure 5. The two molluscan hemocyanins from *Octopus* and *Busycon* exhibit almost identical frequencies and relative intensities, with a dominant feature at 270 cm^{-1} . The arthropod Hc from *Limulus* exhibits a somewhat different set of frequencies and intensities, with its dominant feature at 286 cm^{-1} . The RR pattern for *Limulus* Hc appears to be characteristic of arthropod Hcs, as a similar spectrum has been observed for Hc from the crab *C. magister*.¹⁹

The Cu and D substitution experiments have been repeated for *Busycon* Hc in order to obtain higher resolution RR spectral data. Upon substitution of ^{65}Cu for ^{63}Cu , the peaks at 229, 270, 293, 314, and 345 cm^{-1} shift by -2 , -2 , -2 , -2 , and -1 cm^{-1} , respectively (Figure 6, Table 1). Thus, all of these modes must have Cu–L stretching character. Upon incubation in D_2O , the peaks at 229, 270, 314, and 345 cm^{-1} undergo shifts of -1 , -1 , -2 , and -1 cm^{-1} , respectively (Figure 7, Table 1). Thus, four of the $\nu(\text{Cu}\text{-L})$ modes identified above are likely to have significant Cu–N(His) stretching character.

To gain further information on the nature of the low-frequency vibrations, the effects of $^{18}\text{O}_2$ and H_2^{18}O were also examined. For *Octopus* Hc prepared with $^{18}\text{O}_2$, none of the well-resolved features between 174 and 345 cm^{-1} revealed any oxygen isotope dependence (Table 1). Furthermore, no isotope shifts were observed for *Busycon* Hc in H_2^{18}O (Table 1), even though it had been cycled through the deoxy state in H_2^{18}O . In contrast, aconitase, which has a hydroxyl group coordinated to the Fe_4S_4 cluster, does exhibit H_2^{18}O -dependent isotope shifts for several of its $\nu(\text{Fe}\text{-S})$ modes.³⁵ The complete lack of any H_2^{18}O dependence in either the ν -

(34) Baldwin, M. J.; Ross, P. K.; Pate, J. E.; Tyeklár, Z.; Karlin, K. D.; Solomon, E. I. *J. Am. Chem. Soc.* 1991, 113, 8671–8679.

(35) Kilpatrick, L. K.; Kennedy, M. C.; Beinert, H.; Czernuszewicz, R. S.; Spiro, T. G. *J. Am. Chem. Soc.* 1994, 116, 4053–4061.

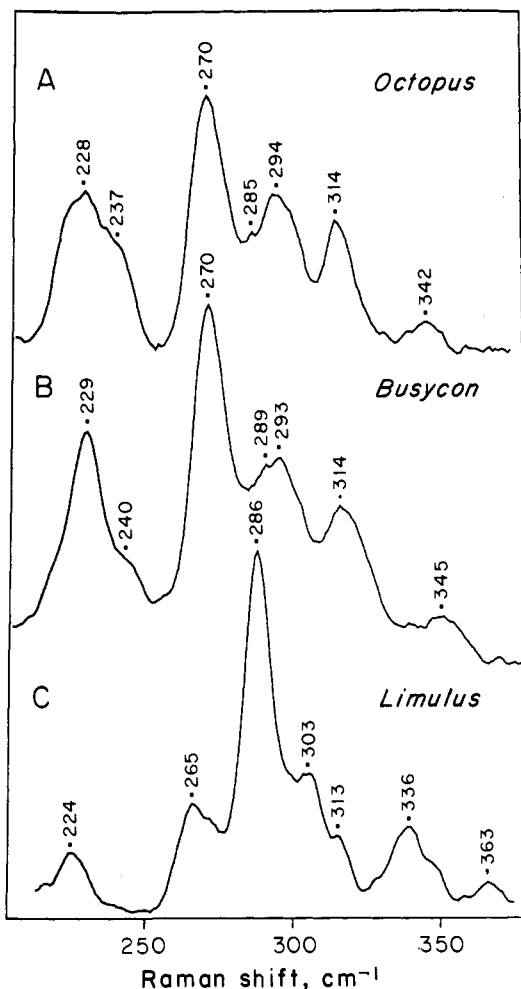


Figure 5. Low-frequency RR spectra of oxyHc from (A) *Octopus*, (B) *Busycon*, and (C) *Limulus*. Spectral conditions and protein concentrations as in Figure 3 except that the spectral resolution and repetitive scanning are as follows: (A) 6 cm^{-1} , 4 scans; (C) 5 cm^{-1} , 10 scans.

(Cu–N), $\nu(\text{Cu}_2\text{O}_2)$, or $\nu(\text{O–O})$ vibrational modes of *Busycon* oxyHc suggests that there are no aqua or hydroxo ligands in molluskan oxyHc.

Normal Coordinate Analysis. Knowledge of the Cu-site geometry in oxyHc makes it worthwhile to utilize normal coordinate analysis (NCA) to assign the vibrational spectrum. An NCA using a simple four-body Cu_2O_2 model has already been performed in conjunction with a vibrational spectroscopic analysis of the $\mu\text{-}\eta^2\text{-}\eta^2$ complex $[\text{CuHB}(3,5\text{-Ph}_2\text{pz})_3]_2(\text{O}_2)$.¹¹ This work led to the prediction of a $\nu_{\text{as}}(\text{Cu}_2\text{O}_2)$ mode at 574 cm^{-1} and was supported by the detection of $2\nu_{\text{as}}(\text{Cu}_2\text{O}_2)$ at 1144 cm^{-1} (Table 1). We have undertaken a more detailed NCA using a $\text{Cu}_2\text{O}_2\text{-}(\text{Im})_6$ model for oxyHc based on our discovery of a $\nu_{\text{as}}(\text{Cu}_2\text{O}_2)$ fundamental at ~ 545 cm^{-1} (Figure 3), improved resolution of the low-frequency vibrational modes (Figure 5), and more accurate information on Cu, D, and O isotope dependence (Figures 6 and 7). The model for this NCA uses the Cu-site geometry and bond distances from the crystal structure of *Limulus* oxyHc,⁸ as reported in Table 2. This model contains a planar Cu_2O_2 unit with four equatorial imidazoles (N_{eq}) and two axial imidazoles (N_{ax}), and each of the imidazoles is treated as a point mass of 67. The model is further constrained to have C_{2h} symmetry with the C_2 axis lying along the O–O bond.

The normal mode calculation was performed using the Wilson GF matrix method²⁵ and a general valence force field including interaction terms. The force constants were refined against a total of 37 observed Raman frequencies, including all the different isotopically labeled forms of *Busycon* oxyHc (Table 1). This

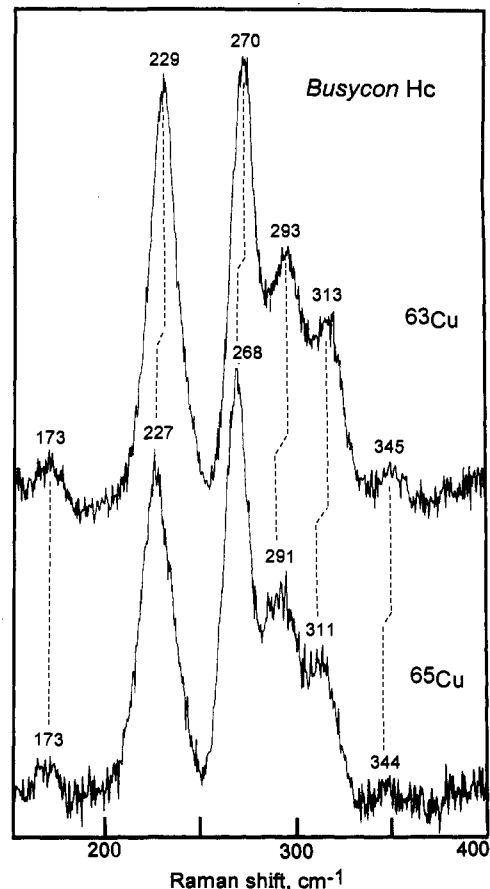


Figure 6. RR spectra of *Busycon* oxyHc reconstituted with ^{63}Cu or ^{65}Cu . Hc samples (2–4 mM in Cu) were in 0.026 M sodium borate, 0.5 M sodium cacodylate (pH 8.5) at 77 K. Spectra were obtained on a Spex instrument using 356.4-nm excitation (50 mW), 10- cm^{-1} slit width, 2 s of counting per 0.5- cm^{-1} increment, and 10 scans.

refinement was performed using an improved algorithm.²⁷ The valence bending and torsion force constants were held constant in order to keep the full rank of the F matrix, and only the remaining 16 of the 23 nonzero force constants were allowed to vary. The resultant force constants are listed in Table 2. These parameters are consistent with literature values for metal–ligand bonds where bending force constants can have up to 30% of the magnitude of stretching force constants.³⁶ A number of interaction force constants were required to obtain adequate fits including all of the frequencies from isotopically substituted samples. These interactions are related to the extensive coupling of Cu–O and Cu–N motions, an unusual feature which may be characteristic of a $\mu\text{-}\eta^2\text{-}\eta^2$ copper peroxide complex.

An NCA was also performed for the *Limulus* Hc data in Table 1, assuming a set of isotope shifts similar to those for *Busycon* Hc. Calculated frequencies and potential energy distributions (PEDs) are given in Table 3. A simplified set of common assignments is listed in Table 1. Displacement coordinates (eigenvectors) for the normal modes of the $\text{Cu}_2\text{O}_2(\text{Im})_6$ moiety in *Busycon* Hc are shown in Figure 8.

(36) Nakamoto, K. *Infrared and Raman Spectra of Inorganic and Coordination Compounds*, 4th ed.; Wiley: New York, 1986.

(37) Yachandra, V. K.; Hare, J.; Gewirth, A.; Czernuszewicz, R. S.; Kimura, T.; Holm, R. H.; Spiro, T. G. *J. Am. Chem. Soc.* **1983**, *105*, 6462–6468.

(38) Loehr, T. M. In *Oxygen Complexes and Oxygen Activation by Transition Metals*; Martell, A. E., Sawyer, D. T., Eds.; Plenum: New York, 1988; pp 17–32.

(39) We have recently found $\nu(\text{N–N})$ in a $\mu\text{-}\eta^2\text{-}\eta^2$ dinitrogen complex of zirconium at the unprecedented value of 731 cm^{-1} , indicating an anomalously low N–N bond order as compared with $\nu(\text{N–N})$ of hydrazine at 1111 cm^{-1} . Cohen, J. D.; Mylvaganam, M.; Fryzuk, M. D.; Loehr, T. M. Manuscript submitted to *J. Am. Chem. Soc.*

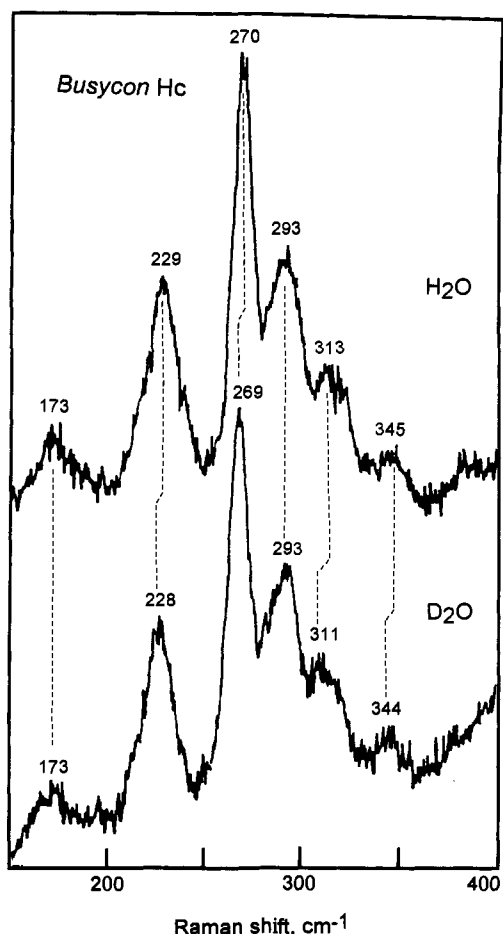


Figure 7. RR spectra of *Busycon* oxyHc incubated in H₂O or D₂O. Hc samples (2–4 mM in Cu) were in 0.05 M sodium carbonate, 0.5 M sodium cacodylate (pH 9.8), and 50% glycerol. Spectral conditions as in Figure 6, except for a 5-cm⁻¹ slit width.

The observed frequencies and isotope shifts for oxyHc from both *Busycon* and *Limulus* are accurately reproduced by our NCA calculations (Table 3). In addition to identifying four of the five predicted stretching modes for a Cu₂O₂ core, we are also able to identify all of the stretching modes predicted for an (N_{eq})₄(N_{ax})₂ ligand set. The substantial Raman intensities for the symmetry-forbidden A_u and B_u modes indicate that the protein environment reduces the effective symmetry of the cluster. This

Table 2. Data Used for Normal Mode Analysis

internal coordinate ^a	<i>Limulus</i> Hc geometry ^b	force constant ^c	
		<i>Busycon</i> Hc	<i>Limulus</i> Hc
bond length			
<i>K</i> (stretching)			
O–O (a)	1.40	2.530	2.412
Cu–O (b)	1.93	1.557	1.533
Cu–N _{eq} (c)	2.05	1.793	1.886
Cu–N _{ax} (d)	2.40	1.079	1.453
bond angle			
<i>H</i> (bending) ^d			
N _{eq} –Cu–N _{eq} (e)	96.5	0.330	0.330
N _{eq} –Cu–N _{ax} (f)	111.0	0.130	0.130
N _{eq} –Cu–O ^e (g)	101.5	0.250	0.250
N _{ax} –Cu–O (h)	99.0	0.220	0.220
torsion angle			
τ (torsion) ^d			
Cu–O ₂ –Cu (i)	180	0.170	0.170
<i>F</i> (stretch–stretch)			
a + b		0.018	0.067
b + c		0.073	0.026
b + d		–0.162	–0.127
c + d		0.217	0.274
<i>F</i> (stretch–bend)			
a + g		0.160 ^d	0.160 ^d
a + h		0.041 ^d	0.041 ^d
b + g		–0.112	–0.102
b + h		–0.080	–0.159
d + f		–0.153	–0.218
d + h		–0.118	–0.172
c + e		0.006	–0.030
c + f		0.179	0.236
c + g		0.163	–0.011
c + h		0.037	0.075

^a N_{eq} = equatorial His; N_{ax} = axial His. Each His treated as an imidazole with a point mass of 67. Interactions of internal coordinates (for example, O–O stretch (a) and Cu–O stretch (b)) are indicated by a + b etc. ^b Based on bond lengths in Å and angles in deg from X-ray crystal structure of *L. polyphemus* oxyHc at 2.4-Å resolution from ref 8. ^c *K* in mdyn/Å, *H* and τ in mdyn·Å/rad², *F* interaction constants in mdyn/Å. ^d Fixed values. ^e The N_{eq}–Cu–O angle to the nearer oxygen of peroxide. The N_{eq}–Cu–O angle of 133.5° to the more distant oxygen has been neglected because its effect is insignificant.

type of enhancement of forbidden modes has been previously observed in RR spectra of other metalloproteins such as the Fe₂S₂-(Cys)₄ cluster in ferredoxin.³⁷ The fact that oxyHcs from two different phyla (*Busycon* and *Limulus*) exhibit the same set of vibrational frequencies and intensities, with only small shifts to higher or lower energy, implies that their Cu-site structures are

Table 3. Calculated Frequencies and Isotope Shifts for Stretching Vibrations in Oxyhemocyanins^a

<i>Busycon</i> Hc		$\Delta^{18}\text{O}_2^b$		$\Delta^{65}\text{Cu}$		ΔD		<i>Busycon</i> PED ^c	<i>Limulus</i> Hc		<i>Limulus</i> PED ^c
obs	calc	obs	calc	obs	calc	obs	calc		obs	calc	
A_g Modes											
749	749.5	40	41.9	0	0.2	0	0.0	O–O(94)	744	744.3	O–O(90)
345	345.6	0	0.4	1	3.0	1	0.9	Cu–N _{eq} (45) + Cu–O(36)	363	363.7	Cu–N _{eq} (57) + Cu–O(24)
270	270.1	0	0.0	2	2.0	1	1.3	Cu–N _{ax} (60) + Cu–N _{eq} (37)	286	286.1	Cu–N _{ax} (84)
174	173.6	0	0.0	0	0.3	0	2.0	Cu–O(30) + Cu–N _{ax} (30)	190	190.7	Cu–N _{eq} (33) + Cu–O(28)
B_g Modes											
547	549.0	23	29.6	0	0.3	0	0.0	Cu–O(99)	543	544.3	Cu–O(98)
289	290.1		0.7	2	1.5		2.0	Cu–N _{eq} (112)	313	311.8	Cu–N _{eq} (101)
A_u Modes											
314	313.0	0	1.9	2	2.0	2	1.4	Cu–N _{eq} (87) + Cu–O(23)	336	337.6	Cu–N _{eq} (76) + Cu–O(21)
240	236.8		10.2		0.0		0.9	Cu–O(56) + Cu–N _{eq} (22)	224	226.3	Cu–O(57) + Cu–N _{eq} (30)
B_u Modes											
	601.2		25.0		1.7		0.1	Cu–O(98)		606.6	Cu–O(93)
293	293.6	0	0.8	2	1.7	0	1.8	Cu–N _{eq} (91)	303	303.7	Cu–N _{eq} (63) + Cu–N _{ax} (40)
229	229.2	0	1.0	2	1.0	1	1.8	Cu–N _{ax} (80)	265	265.4	Cu–N _{ax} (52) + Cu–N _{eq} (27)

^a Observed *Busycon* and *Limulus* Hc frequencies and *Busycon* Hc isotope shifts (all to lower energy) from Table 1. Input geometry from *Limulus* Hc (Table 2). Force constants (Table 2) were refined against the observed frequencies and isotope shifts using an improved algorithm.²⁷ ^b Observed isotope shifts for *Busycon* and *Octopus* Hcs from Table 1. ^c Calculated PED with respect to the independent GVFF constants. Cu–O, Cu–N_{eq}, and Cu–N_{ax} refer to motions of the Cu₂O₂, [Cu(N_{eq})₂]₂, and [Cu(N_{ax})₂]₂ moieties, respectively. Only PED contributions >20% are shown.

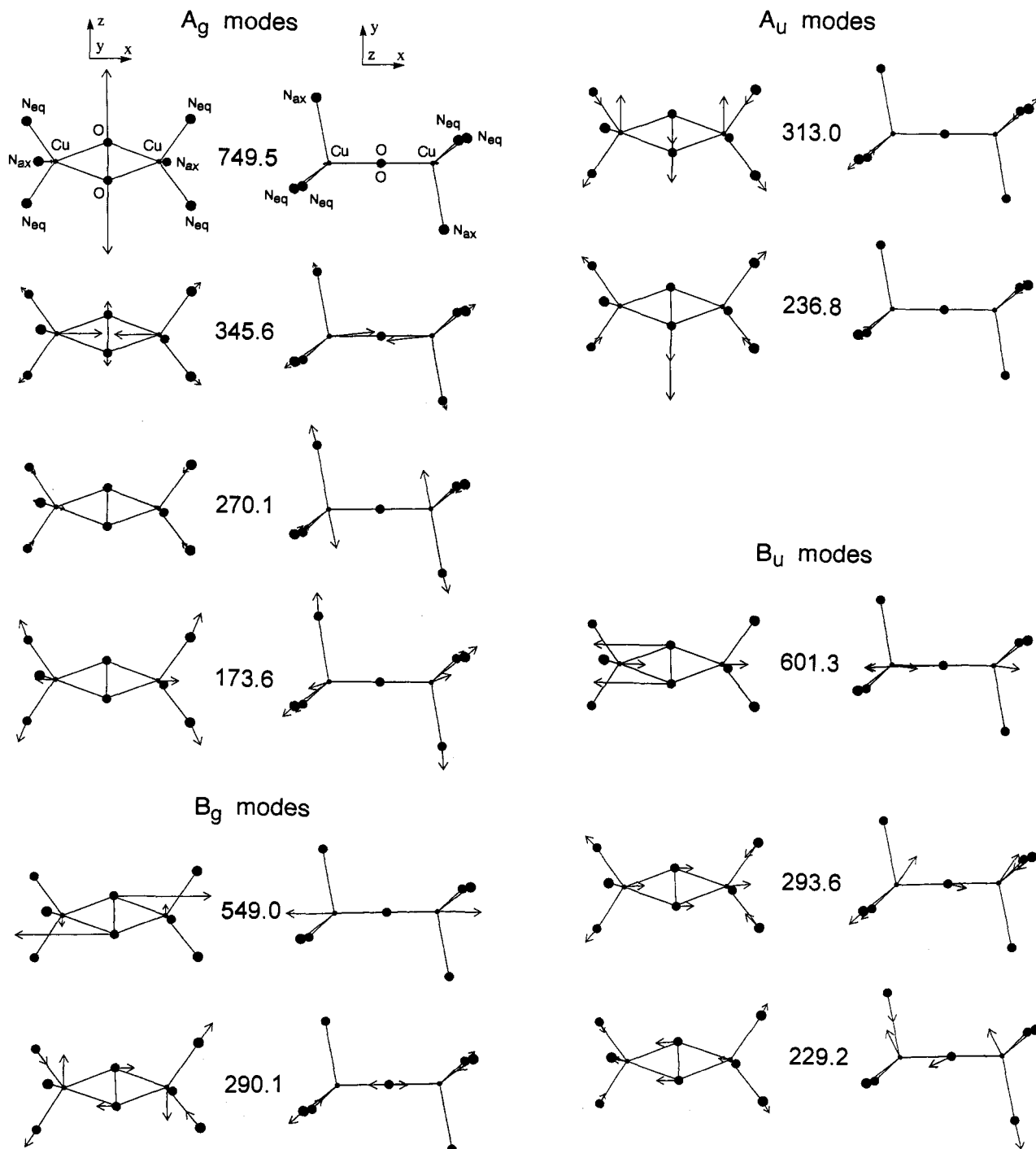


Figure 8. Eigenvectors and calculated frequencies for the A_g , B_g , A_u , and B_u stretching modes of the $\text{Cu}_2\text{O}_2(\text{Im})_6$ cluster in *Busycon* oxyHc assuming a $\mu\text{-}\eta^2\text{:}\eta^2$ coordination geometry and C_{2h} symmetry (based on data in Tables 2 and 3). Two views are shown for each mode. The arrows correspond to unit displacements of normal coordinates using a scaling factor of 20 in all cases except for the O–O stretch, which has a scaling of 15.

quite similar. Interestingly, the $\mu\text{-}\eta^2\text{:}\eta^2$ model compound (Table 1) also displays a number of RR modes between 200 and 320 cm^{-1} , although only the A_g fundamentals have been assigned.¹¹

(a) O–O Stretch. The calculated values for $\nu(\text{O–O})$ at ~ 750 cm^{-1} and for its isotope shift of ~ 40 cm^{-1} in $^{18}\text{O}_2$ (Table 3) are close to the observed frequencies in oxyHcs from all three species (Table 1). The PED reveals that the fundamental mode is almost a pure O–O stretching vibration (Figure 8). The fact that $\nu(\text{O–O})$ is 5 cm^{-1} higher in molluscan (*Busycon* and *Octopus*) than in arthropod (*Limulus* and *C. magister*⁴) Hcs indicates a somewhat stronger O–O bond in molluscan oxyHcs. Nevertheless, the $\nu(\text{O–O})$ frequencies for all oxyHcs and $\mu\text{-}\eta^2\text{:}\eta^2$ model compounds are 50–100 cm^{-1} lower than typical values (800–850

cm^{-1}) for end-on or side-on peroxide complexes in which each oxygen is coordinated to a single metal.^{31,34,38} Thus, a significantly weakened O–O bond appears to be characteristic of side-on peroxides in which both oxygens are coordinated to two metals.³⁹

(b) Cu_2O_2 and Cu– N_{eq} Stretching Modes. The four Cu–O bond stretches account for four modes of A_g , A_u , B_g , and B_u symmetry (Table 3, Figure 8). The B_g and B_u modes calculated at 549.0 and 601.3 cm^{-1} , respectively, involve O atom motion parallel to the Cu...Cu direction and are essentially pure Cu–O stretching in character. The B_u mode is apparently not enhanced (loss of the C_{2h} center of symmetry is required for activation), although a weak 570- cm^{-1} band in the *Limulus* Hc spectrum (Figure 3) is a possible candidate. The ^{18}O -sensitive RR band observed at

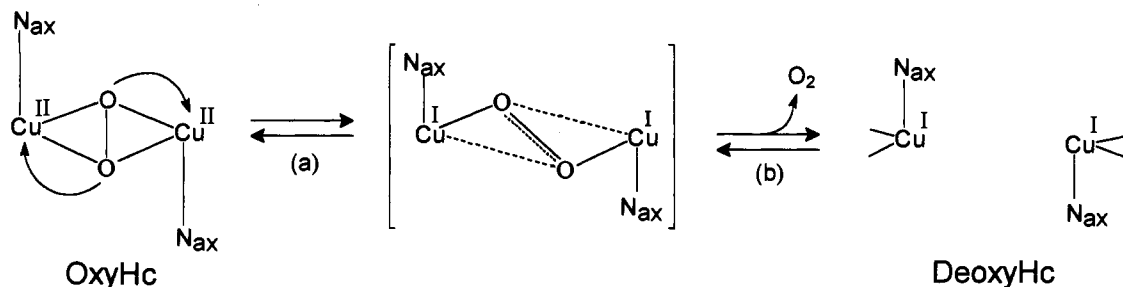


Figure 9. Proposed changes in Cu-site geometry of oxyHc accompanying (a) the 350-nm peroxide \rightarrow Cu(II) charge-transfer transition and (b) the loss of O_2 to form deoxyHc. The axial imidazoles (N_{ax}) are orthogonal to the Cu_2O_2 plane.

$\sim 545\text{ cm}^{-1}$ is assigned to the B_g mode. It is likely that this mode is enhanced by a symmetry lowering in the protein which results in displacement of the excited state along the B_g coordinate, particularly since this mode is not detected in the $\mu\text{-}\eta^2\text{:}\eta^2$ model compound.¹¹

The A_g and A_u modes are expected at much lower frequencies and for the Cu_2O_2 unit were calculated at $\sim 300\text{ cm}^{-1}$.¹¹ The A_g mode involves in-phase motion of the Cu atoms against the O_2 group, which remains essentially motionless (Figure 8). The reduced mass is therefore the full mass of the Cu atom, accounting for the low frequency and lack of ^{18}O dependence. For the A_u mode, the low frequency is due to the O_2 group moving as a unit perpendicular to the $Cu\cdots Cu$ axis (Figure 8). In the $Cu_2O_2(Im)_6$ complex, both the A_g and A_u modes interact strongly with the $Cu-N_{eq}$ modes of the same symmetry because the $Cu-O$ and $Cu-N_{eq}$ bonds are nearly in-line and because their natural stretching frequencies are close in energy. For example, the frequencies of the nearly pure $Cu-N_{eq}$ modes of B_g and B_u symmetry are observed at 289 and 293 cm^{-1} , respectively, in *Busycon* Hc (Table 3).

The strong configuration interaction of the $Cu-O$ and $Cu-N_{eq}$ vibrational energy levels leads to widely split pairs of bands. A pair of A_g modes is observed at 345 and 175 cm^{-1} for *Busycon* Hc and at 363 and 190 cm^{-1} for *Limulus* Hc. Similarly, the A_u pairs are at 314 and 240 cm^{-1} for *Busycon* Hc and at 336 and 224 cm^{-1} for *Limulus* Hc. The $Cu-O$ stretching contribution is equal for the two A_g modes. However, for the A_u pair, the lower member has the larger $\nu(Cu-O)$ contribution as well as a larger expected $^{18}O_2$ shift of 10 cm^{-1} (Table 3). The *Busycon* Hc spectrum does show a weak 240- cm^{-1} band which appears to shift under the stronger 229- cm^{-1} band in the $^{18}O_2$ adduct (data not shown). Interestingly, the $\mu\text{-}\eta^2\text{:}\eta^2$ model compound¹¹ shows a 10- cm^{-1} shift for an infrared band at 331 cm^{-1} , where the higher member of the A_u pair is found in *Limulus* Hc. Perhaps mode mixing is slightly altered in the model compound and shifts the majority of the $\nu(Cu-O)$ character into the higher member of the pair.

Although totally symmetric modes are generally strong, it is of interest that the $Cu-O$ -containing A_g modes of oxyHc are actually quite weak. Indeed, they are substantially weaker than the 545- cm^{-1} B_g mode (Figure 3). We believe that this apparent discrepancy is an indication of the asymmetric character of the excited state. Assuming that the charge-transfer transition is localized and shifts an electron from the bond peroxide to one Cu(II) ion or the other, then the change in geometry between the ground state and the excited state (Figure 9, reaction a) matches the displacement of atoms along the B_g coordinate (Figure 8). Thus, a strong RR enhancement of this mode is expected (provided the protein lowers the symmetry from C_{2h}). The Cu(I)-like excited state in Figure 9 also suggests a mechanism for O_2 binding to deoxyHc. The incoming O_2 initially bridges the 4.6- \AA $Cu\cdots Cu$ distance of deoxyHc in an end-on $\mu\text{-}\eta^1\text{:}\eta^1$ fashion (reaction b) and then rearranges to the symmetrical $\mu\text{-}\eta^2\text{:}\eta^2$ structure of oxyHc, contracting the $Cu\cdots Cu$ distance to 3.6 \AA .

(c) **$Cu-N_{ax}$ Stretching Modes.** The two axial imidazole ligands contribute two $Cu-N_{ax}$ stretching modes of symmetry A_g and B_u . These are assigned, respectively, to the prominent RR bands at 270 and 229 cm^{-1} in *Busycon* Hc and at 286 and 265 cm^{-1} in *Limulus* Hc. These bands show clear ^{65}Cu and D_2O shifts, and they are accurately calculated with force constants that are physically reasonable (Table 2). The resulting force constants for $\nu(Cu-N_{ax})$ are 0.4–0.7 $mdyn/\text{\AA}$ lower than for $\nu(Cu-N_{eq})$, consistent with the relative bond strengths in typical Cu(II) complexes. They are also in agreement with the crystal structure of *Limulus* oxyHc where the average $Cu-N_{ax}$ bond distance of 2.40 \AA is significantly longer than the $Cu-N_{eq}$ bond distance of 2.05 \AA (Table 2). The axial His force constant of 1.08 $mdyn/\text{\AA}$ for *Busycon* Hc is noticeably lower than the value of 1.45 $mdyn/\text{\AA}$ for *Limulus* Hc and thereby accounts for most of the differences in their low-frequency RR spectra (Figure 5).

It is striking that the strongest RR band with near-UV excitation is the A_g mode of the axial ligands at $\sim 270\text{ cm}^{-1}$ in molluscan Hcs and $\sim 285\text{ cm}^{-1}$ in arthropod Hcs. Since the axial bonds are long and weak, a low Raman intensity might ordinarily have been expected. The key to this seeming paradox lies in the fact that, according to the *Limulus* Hc crystal structures,⁸ the axial bonds shorten by 0.4 \AA when oxyHc is deoxygenated. The Cu(II) ions of oxyHc are tetragonal with elongated axial bonds, whereas the Cu(I) ions of deoxyHc are trigonally coordinated via three equally strong bonds. Since the Cu(II) is reduced to Cu(I) in the charge-transfer transition, it is expected that the axial bonds shorten substantially in the excited state (Figure 9), thereby producing a large enhancement of the A_g $Cu-N_{ax}$ stretching mode. We note that the strong 284- cm^{-1} band of the $\mu\text{-}\eta^2\text{:}\eta^2$ model compound $[CuHB(3,5\text{-}Ph_2pz)_3]_2(O_2)$ (Table 1) is likely to be the A_g axial pyrazole mode, rather than the previously suggested A_g $Cu-O$ mode.¹¹ The axial pyrazole bonds at 2.26 \AA in the *i*- Pr_2pz form of this complex¹⁰ are likewise appreciably longer than the 2.00- \AA equatorial pyrazole bonds.

Our model of a $Cu_2O_2(Im)_6$ cluster with C_{2h} symmetry provides an excellent fit to the observed vibrational modes and isotope shifts in both molluscan and arthropod Hcs (Table 3) as well as the observed bond distances in the crystal structure of *Limulus* oxyHc.⁸ These results suggest that the Hcs from both phyla have six terminal His ligands at the dinuclear Cu site. For molluscan Hc, three His have been identified as ligands for the Cu B site on the basis of sequence similarity with arthropod Hcs.¹⁵ Another three His have been suggested as ligands for the Cu A' site on the basis of sequence similarity with tyrosinases.¹⁷ The RR spectrum of oxytyrosinase from *Neurospora crassa*⁴⁰ exhibits equally enhanced $\nu(Cu-N_{ax})$ modes and an equally low frequency for $\nu(O-O)$. This is strong evidence for the same $\mu\text{-}\eta^2\text{:}\eta^2$ peroxide configuration in oxytyrosinases and oxyhemocyanins. In contrast, arthropod Hcs from *C. magister*, *Cancer irroratus*, and *Cancer borealis*¹⁹ have their $\nu(Cu-N_{ax})$ modes at 282, 288, and 284 cm^{-1} , respectively, which are closer in energy to the 286- cm^{-1}

(40) Eickman, N. C.; Solomon, E. I.; Larrabee, J. A.; Spiro, T. G.; Lerch, K. *J. Am. Chem. Soc.* 1978, 100, 6529–6531.

value for *Limulus* Hc. The stronger Cu–N_{ax} bonds in arthropod Hcs may also be responsible for their slightly lower O–O bond strengths.

The 2-thioether imidazole modification of one of the proposed His ligands in the CuA' site has been observed for both molluskan Hc and *N. crassa* tyrosinase.¹⁷ Our studies suggest that this modified His ligand is more weakly coordinated and in an axial position, thereby contributing to the low $\nu(\text{Cu-N}_{\text{ax}})$ value of 270 cm⁻¹ in *Busycon* Hc. Supporting evidence comes from the RR spectra of other molluskan Hcs and *N. crassa* tyrosinase. Similar low frequencies for $\nu(\text{Cu-N}_{\text{ax}})$ are observed at 270 cm⁻¹ for *Limulus* Hc, 267 cm⁻¹ for *Megathura crenulata* Hc,¹⁹ and 274 cm⁻¹ for *N. crassa* tyrosinase.⁴⁰ In contrast, arthropod Hcs from *C. magister*, *Cancer irroratus*, and *Cancer borealis*¹⁹ have their $\nu(\text{Cu-N}_{\text{ax}})$ modes at 282, 288, and 284 cm⁻¹, respectively, which are closer in energy to the 286-cm⁻¹ value for *Limulus* Hc. The stronger Cu–N_{ax} bonds in arthropod Hcs may also be responsible for their slightly lower O–O bond strengths.

The variation in the bond lengths of the axial His ligands may have physiological significance. A comparison of the crystal structures of two arthropod deoxyHcs reveals interesting differences with respect to the axial His ligands.^{8b,c} The crystal structure of *Panulirus* deoxyHc at low pH shows a marked lengthening of the Cu–N_{ax} bonds to 2.7 Å, compared to 2.0 Å for *Limulus* deoxyHc at neutral pH. The longer bond length in the *Panulirus* protein is believed to be due to imidazole protonation.^{8c} In addition, the *Panulirus* low-pH structure shows a Cu...Cu distance of 3.5 Å compared to 4.6 Å for *Limulus* deoxyHc which is in the low-affinity T state. The shorter Cu...Cu distance in the *Panulirus* protein suggests that the elongation of Cu–N_{ax} upon protonation has forced the protein into the high-affinity R state conformation. Thus, O₂ affinity of Hc may be modulated by the length of the axial imidazole bond.⁸ The strong $\nu(\text{Cu-N}_{\text{ax}})$ mode of oxyhemocyanins at 270–286 cm⁻¹ may prove useful as a monitor of R and T conformations, much like the Fe–N(His) mode in the RR spectra of deoxyhemoglobins.⁴¹

Conclusions

1. Hemocyanins from arthropods and mollusks bind O₂ in the same fashion, producing a $\mu\text{-}\eta^2\text{:}\eta^2$ cupric peroxide. This assessment is based on the similarity of their electronic and RR spectra. In particular, oxyHcs from arthropods and mollusks exhibit an abnormally low $\nu(\text{O-O})$ at ~ 745 cm⁻¹, which is similar to the 741-cm⁻¹ value for the $\mu\text{-}\eta^2\text{:}\eta^2$ model compound¹⁰ but 50–100 cm⁻¹ lower than the values for other metal peroxide complexes.

(41) Nagai, K.; Kitagawa, T.; Morimoto, H. *J. Mol. Biol.* **1980**, *136*, 271–289.

Another hallmark of the $\mu\text{-}\eta^2\text{:}\eta^2$ structure is the resonance enhancement of $\nu_{\text{as}}(\text{Cu}_2\text{O}_2)$ at ~ 545 cm⁻¹, as well as its overtone at ~ 1090 cm⁻¹. Neither of these vibrational modes has been observed in any other type of peroxide complex, but they are observed in arthropod and molluskan Hcs and in the $\mu\text{-}\eta^2\text{:}\eta^2$ model compound.

2. Neither $\nu(\text{O-O})$ nor $\nu_{\text{as}}(\text{Cu}_2\text{O}_2)$ shows any deuterium isotope sensitivity, making it unlikely that the low energy of $\nu(\text{O-O})$ is due to hydrogen bonding. The weakening of the O–O bond is rather a consequence of the unusual coordination of each oxygen by two metals. It has been proposed that these side-on complexes have weaker O–O bonds because they allow greater metal ion back-donation into antibonding orbitals.¹¹

3. The entire vibrational spectrum (including the eight vibrational modes between 170 and 370 cm⁻¹) is particularly well described by a normal coordinate analysis using a Cu₂O₂(Im)₆ model with four equatorial N_{eq}, two axial N_{ax}, and C_{2h} symmetry. This analysis indicates that most of the features in the 170–370-cm⁻¹ region are Cu–N_{eq} and Cu–N_{ax} stretching vibrations mixed to various extents with Cu₂O₂ stretching vibrations. The preponderance of the imidazole contribution explains why most of these modes exhibit shifts of –1 to –2 cm⁻¹ upon deuterium substitution.

4. The most intense feature at 270 cm⁻¹ in molluskan Hc and 286 cm⁻¹ in arthropod Hc is assigned to the symmetric stretch of the two N_{ax} ligands. Its strong Raman enhancement is attributed to the fact that the Cu–N_{ax} bonds are the ones that undergo the greatest change in bond lengths in the electronic excited state. A similar assignment is now proposed for the intense 284-cm⁻¹ mode in the $\mu\text{-}\eta^2\text{:}\eta^2$ model compound¹¹ as well as the 274-cm⁻¹ mode in oxytyrosinase,⁴⁰ which is also deemed to have a $\mu\text{-}\eta^2\text{:}\eta^2$ peroxide configuration.

5. The excellent fit of the observed RR spectrum of both molluskan and arthropod Hcs using NCA with a Cu₂O₂(Im)₆ model suggests that molluskan Hc also has six His ligands. The lower energy for the Cu–N_a stretch in molluskan Hcs may be due to one of the axial imidazole ligands being covalently linked to a cysteine thiol.

Acknowledgment. We sincerely thank Drs. Karen Miller and Celia Bonaventura for providing samples of hemocyanin, Drs. Karen Magnus and Gisèle Préaux for making structural data available prior to publication, and Jingyuan Ai for help in protein purification. This research was supported by grants from the National Institutes of Health (Grant GM18865 to T.M.L. and J.S.-L., Grant GM48370 to R.S.C., and Grant GM13498 to T.G.S.).